THE UNIVERSITY of EDINBURGH

Edinburgh Research Explorer

Residual capacity of fire-exposed concrete-filled steel hollow section columns

Citation for published version:
Rush, D, Bisby, L, Gillie, M, Jowsey, A & Lane, B 2015, 'Residual capacity of fire-exposed concrete-filled steel hollow section columns', *Engineering Structures*, vol. 100, pp. 550-563. https://doi.org/10.1016/j.engstruct.2015.06.039

Digital Object Identifier (DOI):
10.1016/j.engstruct.2015.06.039

Link:
Link to publication record in Edinburgh Research Explorer

Document Version:
Peer reviewed version

Published In:
Engineering Structures

General rights
Copyright for the publications made accessible via the Edinburgh Research Explorer is retained by the author(s) and / or other copyright owners and it is a condition of accessing these publications that users recognise and abide by the legal requirements associated with these rights.

Take down policy
The University of Edinburgh has made every reasonable effort to ensure that Edinburgh Research Explorer content complies with UK legislation. If you believe that the public display of this file breaches copyright please contact openaccess@ed.ac.uk providing details, and we will remove access to the work immediately and investigate your claim.

OPEN ACCESS

Download date: 04. May. 2023

RESIDUAL CAPACITY OF FIRE-EXPOSED CONCRETE-FILLED STEEL HOLLOW SECTION COLUMNS

Dr. David I. Rush[a], Prof. Luke A. Bisby[b], Dr. Allan Jowsey[c] and Prof. Barbara Lane[d]

[a] Postdoctoral Research Associate, BRE Centre for Fire Safety Engineering, School of Engineering, University of Edinburgh, UK, d.rush@ed.ac.uk – Corresponding Author
[b] Arup Chair of Fire and Structures, BRE Centre for Fire Safety Engineering, School of Engineering, University of Edinburgh, UK, luke.bisby@ed.ac.uk
[c] Manager, Fire Protection, International Paint Ltd., Gateshead, UK, allan.jowsey@akzonobel.com
[d] Arup Fellow and Visiting Professor of Fire Safety Engineering, University of Edinburgh, UK, barbara.lane@arup.com

ABSTRACT

Concrete filled steel hollow structural (CFS) sections are an increasingly popular means to support large compressive loads in buildings. Whilst the response of unprotected CFS sections during a fire is reasonably well researched, their post-fire residual structural performance is less well established. A better understanding of the response of fire-damaged CFS columns is needed to enable better performance-based structural fire engineering of buildings incorporating CFS sections. This paper presents post-fire residual compression tests on unprotected and protected CFS columns along with control tests on six unheated sections. The tests confirm that as the maximum exposed temperature within the cross-section increases, the residual strength capacity, ductility and axial-flexural stiffness decrease. The data are subsequently used to assess the ability to predict the residual capacity of CFS columns after fires, using available post-fire material models and in-fire and ambient structural models.

Keywords: Fire resistance; concrete filled steel hollow sections; CFS; post-fire residual strength; intumescent coatings; property protection; predictions; columns.

1 INTRODUCTION

Concrete filled steel hollow structural sections (CFS) are hollow steel sections (circular, prismatic, or ovular) that are in-filled with plain or reinforced concrete to provide superior load carrying capacity, and enhanced structural fire resistance, as compared with unfilled steel tubes. They are an attractive, efficient, and relatively environmentally sustainable means (as compared to plain steel or reinforced concrete members) by which to support large compressive loads in multi-storey buildings. The concrete infill and the steel tube work together to share load through composite action at ambient temperatures, but also during a fire and after a fire. The concrete infill enhances the steel tube's resistance to local buckling, and the steel tube provides confinement to the concrete core, thus increasing its load bearing capacity. The steel tube also acts as stay-in-place formwork during construction, reducing forming and stripping costs, and provides a smooth, rugged, architectural surface finish.

A large amount of design guidance is available [e.g. 1, 2] to predict the fire resistance for CFS columns during standard fires. However after a fire, when a building may have not experienced any obvious structural failure, a question arises as to the level of structural damage that may have been sustained, and whether (or how) the building can be safely repaired and put back into use. Such questions are becoming more important, as structural fire engineers, insurers, building developers and tenants begin to factor other performance criteria in addition to life safety, such as property protection, environmental impacts, and business continuity considerations, when making structural fire engineering design decisions. Only limited work is available on the post-fire residual strength of fire-exposed CFS columns [3-5]

This paper presents tests on the post-fire residual compressive load bearing and lateral deformation capacity of 19 CFS columns after being exposed to standard fires and cooled to ambient temperature prior to structural testing to failure. Tests on six unheated control columns are also presented. Parameters varied between tests include the severity and duration of heating, the concrete infill type, the cross-section

shape, the steel wall thickness, and the amount of supplemental fire protection. The data are then used to assess the ability of available post-fire structural and material models [1, 5, 6] to predict the residual capacity of CFS columns after fires.

2 BACKGROUND

Only limited research is available on the residual capacity of fire-exposed CFS columns. Han et al. [3], [5] have presented tests and analysis of more than 40 CFS columns after exposure to fire, and have also suggested complex post-fire material models for use in predicting CFS columns' residual capacity [5]. Han's work includes post-fire residual tests [3], [5] on both protected and unprotected, scaled CFS columns. This work has considered only the standard ISO 834 fire curve [5], or exposure to constant temperatures ranging between 20ºC and 900ºC [4], with tests on both square and circular columns ranging in length between 380 and 1200 mm and with maximum cross-sectional dimensions between 80 and 133 mm. Wall thicknesses between 2.9 and 4.8 mm have been considered. The steel tubes were filled with plain concrete ranging in strength from 35 to 72 MPa. For tests exposed to transient thermal regimes, unprotected specimens were subjected to 90 minutes of exposure to the standard fire, while protected specimens were heated for 180 mins. The majority of the columns were tested under concentric axial load, however a small number had initial load eccentricities of 15 to 18 mm and (as expected) failed at lower loads than otherwise identical concentrically loaded columns.

Taken together, Han et al.'s published work in this area [3-7] has demonstrated that the residual mechanical behaviour of the fire exposed CFS columns under axial load remains ductile (as for ambient unheated tests), and that composite enhancement (i.e. confinement) of the concrete core remains present after heating [3]. The post-heated columns failed in either global buckling of the columns or local buckling of the steel tubes, with accompanying crushing of the concrete core. The fire duration, column section size, and slenderness ratio were observed to have significant effects on the residual strength of the columns, whereas other parameters (steel ratio, concrete strength, and steel strength) had only minor

effects. Unsurprisingly, loss of strength was considerably less for protected sections [4]. Interestingly, it was noted that load eccentricity appeared to be important for the *residual strength index* (RSI) of the columns. The RSI is defined (also herein) as the ratio of the tested strength (N_{test}) to the strength of an identical unheated column ($N_{ambient}$); i.e. RSI = $N_{test}/N_{ambient}$.

Han et al. [5, 6] have devoted considerable effort to developing post-fire residual material models and predictive equations for the RSI of both unprotected and protected (with a specific cementitious protection material) CFS columns after exposure to the standard fire. The material models for concrete and steel make two noteworthy assumptions, namely that: (1) the residual mechanical properties of both steel and concrete depend only on the peak exposure temperature, and are not influenced by the cooling rate, the time since heating, or the relative humidity of the cooling environment (which is known to influence the residual properties of concrete, in particular [8]); and (2) steel tubes in CFS columns provide confinement to the core concrete both before and after fire, and enhance its compressive strength and deformability (more effectively for circular columns). Given the complexity of Han et al.'s formulations, full details of their equations are avoided here and are presented in full in [5, 6]. However, for the purposes of illustration, Figure 1 shows Han et al.'s predicted residual stress versus strain curves for the concrete used in the current study (described in detail in the following sections), when confined within either circular or square CFS sections with the dimensions tested herein, with 5 mm steel wall thickness. These predictions were made for 70 MPa compressive strength concrete. It is noteworthy that Han et al.'s proposed stress-strain relations suggest the same confined compressive strength for concrete in both circular and square columns (which is known not to be the case [9]), however circular columns demonstrate a lower level of post-peak softening as a consequence of the superior lateral confinement in circular versus square CFS sections. Also shown in Figure 1(c) are the Han et al.'s proposed bi-linear post-fire residual stress strain curves for steel.

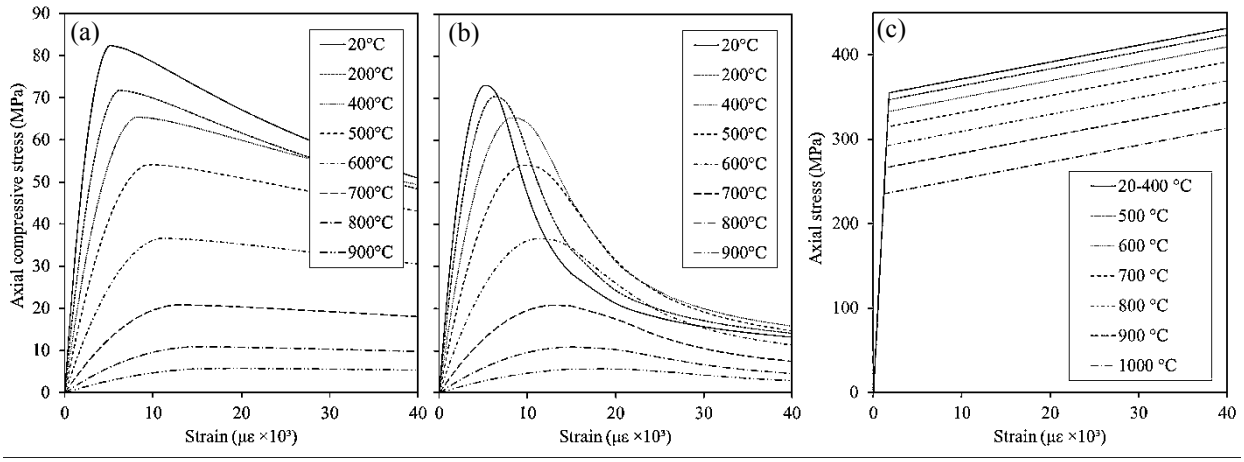

Figure 1 - Predicted [5, 6] **residual stress versus strain curves for the concrete used in the current study when confined in (a) circular or (b) square steel tubes; and (c) predicted stress versus strain response for steel.**

Han and Huo [5] also propose equations for the RSI of unprotected CFS columns exposed various durations of the standard fire, based on a series of numerical parametric studies performed using a plane-sections equilibrium analysis similar to that suggested by Lie et al. [10]. Again, the full details of the equations are avoided here but are given in the source publication [5]. It should be noted, however, that Han and Huo's equations are explicitly limited to section sizes greater than 200mm, with no explanation of the rationale for this limitation. This is seems peculiar since Han and Huo's own testing, upon which their models are based, involved circular 108mm Ø and square 100 x 100 mm sections which were reasonably predicted using their RSI equations. For the purposes of illustration, Figure 2 shows the predicted RSIs for the CFS column geometries tested in the current study (described in the following section). Han and Huo's [5] predictive equations account for column size, shape, and slenderness, but take no account of steel wall thickness, concrete infill type or strength, steel yield strength, or non-standard heating regimes. They are also unable to treat the case of protected columns, making their utility marginal for post-fire assessment (where heating will have been non-standard) or performance-based structural fire engineering design (where fire protection systems such as intumescent coatings are widely used).

As expected, the predicted RSI for both circular and square CFS sections decreases with increasing exposure to the standard fire. For the columns in the current study (see below), an RSI of about 0.37 is predicted for all unprotected sections after 120 minutes of fire exposure.

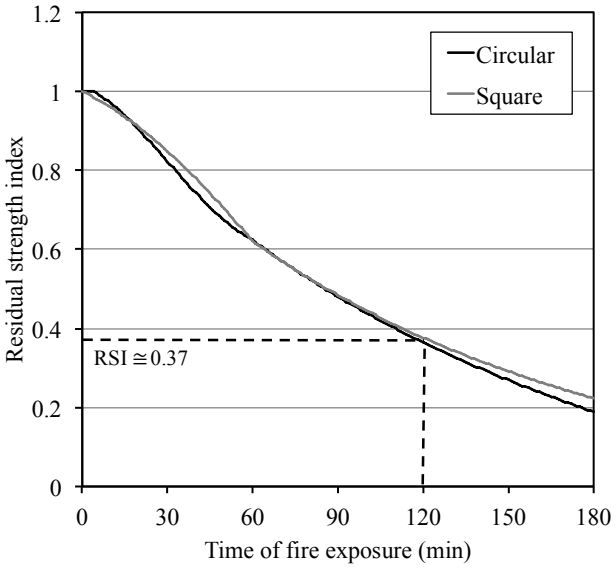

Figure 2 - Predicted [5] RSIs for the unprotected circular and square CFS column geometries tested in the current study when exposed to ISO 834 [11] **standard fire conditions (these are independent of steel wall thickness).**

Han's work provides a basis for understanding the post-fire residual capacity of CFS columns, however the available testing is limited in scope and cannot provide confident validation of the various proposed predictive equations, it considers only standard fire exposures, and is based on CFS sections with plain concrete infill as opposed to fibre reinforced concrete infill – the latter is gaining popularity in the construction industry as it can negate the need for cumbersome, inconvenient, and costly internal steel reinforcement within the infill concrete, while providing adequate fire resistance in many cases. The current study seeks to address these points by extending the database of available test results, and comparing these data against predictions made with the aforementioned models.

3 EXPERIMENTAL PROGRAMME

The experimental programme in the current study involved mildly eccentric axial compressive loading, to failure, of 25 fire-exposed CFS columns. An overview of the tests is provided in Table 1, whereas exhaustive details of the testing program are given by Rush [12]. Nineteen of the specimens were heated for 120 minutes (or 180 minutes in one case) prior to structural testing to assess their residual response, while the remaining six were used as unheated control specimens. Five key parameters were assessed in order to better understand their respective influence on the post-fire residual capacity of CFS sections, namely: (1) cross-section shape, (2) steel tube wall thickness, (3) type of infill concrete, (4) applied fire curve, and (5) the presence of applied protection. Four additional tests were also performed to evaluate the impacts of (6) concrete age at the time of testing, and (7) intumescent coating thickness.

Seven (7) square (denoted as *S*) and eighteen (18) circular (*C*) sections were tested, with steel wall thicknesses being 5, 8 or 10 mm. All columns were 1400 mm in length and were made from Grade S355 (i.e. 355 MPa nominal yield strength) steel. The tubes were filled with high strength (nominally 70 MPa 28-day compressive strength) concrete (denoted as *HSC*) or fibre reinforced concrete (*FIB*). The *FIB* mix differed from the *HSC* mix only in that it incorporated a hybrid steel (Propex Novocon HE 05535) and polypropylene (Propex FM 150 Micro) fibre mix of 45 kg/m^3 and 2 kg/m^3, respectively. Fifteen of the columns were exposed to an ISO 834 (*I*) fire [11] and four were exposed to the Eurocode smouldering (slow-growth) fire (*S*) [13]. These two thermal regimes were selected to advance understanding of the heat transfer in CFS sections, particularly as regards the performance of intumescents under non ISO 834 heating regimes. Section 3.1 describes the full thermal exposure procedure, including the cooling phases, to which the CFS sections were exposed. Eight (8) columns were unprotected and eleven (11) were protected with a thin-film, water-borne intumescent coating sold under the trade name Interchar 1120 (the trade name is stated only for factual accuracy).

The details, dimensions, and material properties of the specimens outlined in Table 1 were selected so that the predicted ambient capacity of the CFS columns was less than the 2000 kN maximum load capacity of the available structural testing equipment. Full details of the fire tests are given, along with full and detailed descriptions of the effectiveness of the intumescent fire protection coating *during* fire, by Rush [12]. In the current paper the key issue is the maximum temperature experienced at any point during the heating and cooling stages at various locations within the column cross-sections; hence these are also given in Table 1 for the steel tube, the outer surface of the concrete core, a depth of 35 mm into the concrete core, and the column centreline.

Table 1: Testing matrix and maximum temperatures recorded in steel tube and concrete core during fire testing.

Test designation[a]	Size (mm)	Wall thick. (mm)	Infill type[b]	Heating regime[c]	FRR[d]	Peak temperature (°C)[e]			
						Steel	Conc. face	35 mm	Conc. cent.
S-10-F-N-N	120	10	*FIB*	*N*	N/A	20	20	20	20
S-5-F-N-N		5	*FIB*	*N*	N/A	20	20	20	20
S-10-F-I-N		10	*FIB*	*I*	N/A	991	969	893	886
S-5-F-I-N		5	*FIB*	*I*	N/A	979	930	856	841
S-5-F-S-N		5	*FIB*	*S*	N/A	988	956	833	826
S-5-F-I-C		5	*FIB*	*I*	90	314	290	281	281
S-5-F-S-C		5	*FIB*	*S*	90	434	383	319	322
C-5-H-N-N	139.7	5	*HSC*	*N*	N/A	20	20	20	20
C-5-F-N-N		5	*FIB*	*N*	N/A	20	20	20	20
C-8-F-N-N		8	*FIB*	*N*	N/A	20	20	20	20
C-10-F-N-N		10	*FIB*	*N*	N/A	20	20	20	20
C-10-F-I-N		10	*FIB*	*I*	N	1005	995	924	871
C-8-F-I-N		8	*FIB*	*I*	N	992	977	913	888
C-5-H-I-N		5	*HSC*	*I*	N	996	952	835	822
C-5-F-I-N		5	*FIB*	*I*	N	997	954	834	820
C-5-F-S-N		5	*FIB*	*S*	N	980	935	787	773
C-10-F-I-C		10	*FIB*	*I*	90	375	358	350	349
C-8-F-I-C		8	*FIB*	*I*	90	389	387	373	361
C-5-H-I-C		5	*HSC*	*I*	90	348	337	319	317
C-5-F-I-C		5	*FIB*	*I*	90	403	397	380	340
C-5-F-S-C		5	*FIB*	*S*	90	380	375	368	366
C-5-F-I-C(14d)	139.7	5	*FIB*	*I*	90	404	371	365	365
C-5-F-I-C(28d)		5	*FIB*	*I*	90	470	452	435	432
C-5-F-I-C(75)		5	*FIB*	*I*	75	608	542	509	514
C-5-F-I-C(120)		5	*FIB*	*I*	120	620	579	568	514

[a] *Naming scheme: Shape – wall thickness – fill type – fire exposure – protection type (age at time of testing or design fire resistance differing from 90 minutes)*, [b] *FIB* = fibre reinforced concrete, *HSC* = high strength concrete, [c] *I* = ISO 834, *S* = smouldering fire, *N* = unheated, [d] FRR = fire resistance design rating, [e] Average maximum temperature at thermocouples.

Temperatures within the columns during fire exposure were recorded at two vertical sections, at approximately $L/3$ and $2L/3$, using K-Type thermocouples (TCs), as shown in Figure 3. All heated columns were exposed to fire for 120 minutes, except in one case where the fire protection was designed to give 120 minutes fire resistance and the test was continued for 180 minutes, after which point the specimens were allowed to cool within the furnace for a further 120 minutes before the furnace doors were opened. The intumescent coating thicknesses for the protected CFS sections were prescribed using current UK guidance [14], with an assumed steel tube limiting temperature of 520ºC and a required fire resistance of 90 minutes (apart from specimens C-5-F-I-C(75) and C-5-F-I-C(120), for which the protection was designed for 75 minutes and 120 minutes, respectively). This approach to fire protection design implies that the limiting temperature of the steel tube should not be exceeded within the required fire resistance period, when subjected to the standard fire [i.e. 12].

3.1 Fire Exposures

The fire exposures were carried out in conventional, ceramic lined standard fire testing furnaces at the AkzoNobel fire protection research and development laboratory in Gateshead, UK. After 120 minutes of heating (or 180 minutes for C-5-F-I-C(120)), the gas supply was halted and data were recorded for a further 120 minutes during cooling. The maximum temperatures experienced by the CFS sections were 1051ºC and 1022ºC for the ISO-834 [11] and smouldering fire curves [13], respectively. All specimens were tested in an unloaded condition.

Due to the limited availability of different testing furnaces a $1.5 \times 1.5 \times 1.8$ m^3 fire testing furnace was used for the tests on C-5-F-I-C(14d) and C-5-F-I-C(28d), the smouldering curve tests x-x-x-S-x, and the tests with variable design fire resistance; C-5-F-I-C(120) and C-5-F-I-C(75). A $4.0 \times 3.0 \times 2.0$ m^3 furnace was used for all other tests. Both furnaces were lined with ceramic tiles, and ceramic wool was placed over the tops and the base plates of the specimens to provide conditions as close as possible to idealized two-dimensional heat transfer within the specimens' cross-sections, as is standard practice for

furnace tests on such elements [16]. Figure 4 shows representative unprotected and protected columns installed in the 1.5 × 1.5 × 1.8 m^3 furnace prior to heating.

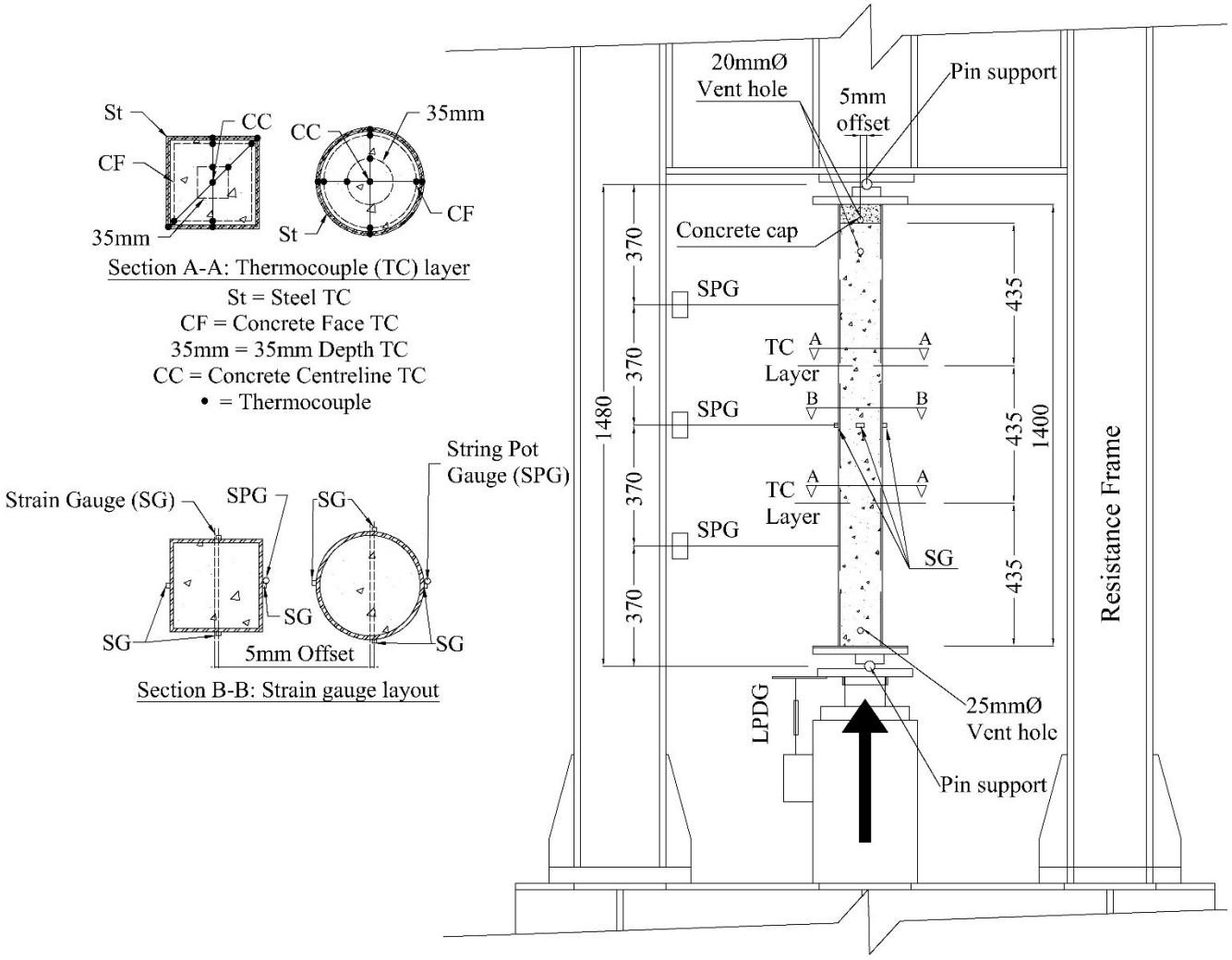

Figure 3 - Schematic of structural testing setup and typical specimen details.

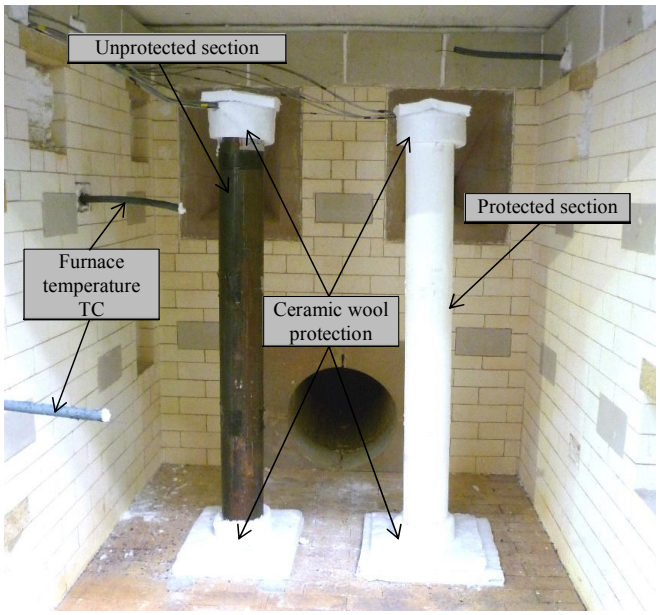

Figure 4 - Representative unprotected (left) and protected (right) CFS columns moments before exposure to heating in the 1.5 × 1.5 × 1.8 m^3 fire testing furnace.

3.2 Structural Testing

During structural testing the columns were attached to pin supported plates at either end, through which a small, essentially arbitrary, initial axial load eccentricity of 5 mm was introduced to the compressive load; this eccentricity controlled the direction of lateral deflection allowing the lateral deflection measurement to be predetermined. An eccentricity of 5 mm is also in accordance with design limits [17] for structural imperfections (i.e. effective length/300). The columns were placed inside a self-reacting structural frame, shown in Figure 3, yielding an effective buckling length of 1480 mm. Bonded electrical resistance foil stain gauges (SGs) were installed on the steel tube evenly around the columns' perimeters at their mid-heights (Section B-B in Figure 3); two of these were placed in line with the pin supports and were placed two perpendicular to the pin supports. Three string pot displacement gauges (SPGs) were attached to the columns at their quarter heights (relative to their effective buckling length) to measure lateral deformations. A linear potentiometer displacement gauge (LPDG) measured axial displacement (stroke) of the hydraulic jack used load the columns, and a pressure gauge was attached in-line with an

electric hydraulic power pack to record load. Tests were performed using an approximate actuator stroke rate of 2.5 to 3.5 mm/min, and were terminated when the rotation of the top or bottom hinge plate was impeded by contact with the actuator or frame due to large rotations.

Since the columns were exposed to fire without the top steel plate attached – so as to permit the internal thermocouples to exit the steel tubes – a small amount of concrete capping (infill) and a top steel plate were added before structural testing could be undertaken. These are shown at the top of the column in Figure 3. High strength concrete mortar was used to fill the steel tubes to their top, and a steel plate was then welded in place. The compressive strength of the concrete fill exceeded 90 MPa at 28 days, thus ensuring that the top region of the columns was stronger than the fire-exposed portions.

4 RECORDED TEMPERATURES

A detailed description of the time histories of temperatures recorded in the various specimens, along with a description of the effectiveness of the intumescent fire protection system used and the consequences for the fire resistance of the specimens *during* fire, is avoided here but is given by Rush [12]. As already noted, the key issue for assessing the residual capacity of the cross-sections – this being the focus of the current work – is the distribution of peak temperatures experienced over the columns' cross sections.

Table 1 gives peak temperatures measured in several locations for each column at any point during the heating and cooling phases of the fire tests. Note that temperatures in the concrete tended to increase for a period during the cooling phase, as expected, due to the thermal wave continuing to move through the cross sections [18]. At the column centreline, for instance, peak temperatures continued to increase as much as 90^{o}C twenty-five minutes into the cooling phase for unprotected columns, whereas for protected columns peak temperatures during cooling were up to 180^{o}C greater than at the end of the heating phase and in some cases occurred more than 100 minutes into cooling.

For illustration, Figure 5 shows representative temperatures experienced within unprotected and protected circular and square CFS columns during the furnace tests. This figure shows that the

unprotected sections experienced very high temperatures in all locations, with temperatures even at the column centerline generally exceeding 800ºC. With reference to Figure 1a-b, exposure to temperatures in this range can be expected to seriously damage (e.g. up to 80-90% reduction) the concrete core's ability to carry load [17, EN1992-1-2], and in these columns it is expected that the majority of the residual load carrying capacity would be due to the steel tube, which can be expected to regain as much as 65% of its ambient temperature strength after cooling from temperatures as high as 1000 ºC (Figure 1c) [18, EN 1993-1-2].

Figure 5 also shows that the intumescent paint fire protection was extremely effective in providing fire protection to the CFS columns, with peak temperatures generally less than 400ºC at all measurement locations. Protected columns can therefore be expected to retain the vast majority of their ambient capacity post-fire [7]. Protected columns also demonstrate more uniform peak temperatures over their cross-section, this being a result of the lower heating rates and hence lower thermal gradients in these sections – these can be expected to reduce the severity of differential thermal stresses in the protected sections, and may contribute to further enhanced post-fire residual capacity. Neither the cross-section shape, nor steel tube wall thickness, nor type of infill concrete, nor applied fire curve obviously influenced the peak temperatures experienced in the columns.

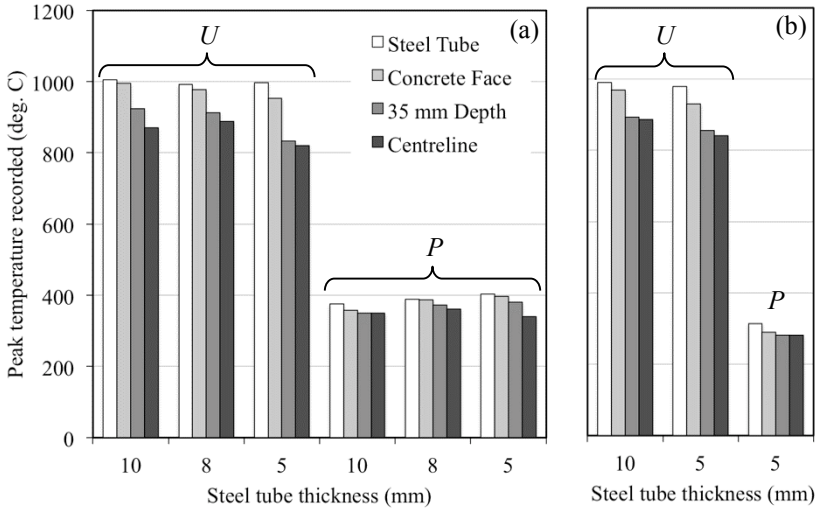

Figure 5 - Representative temperatures experienced within typical unprotected and protected (a) circular and (b) square CFS columns during unloaded furnace tests (*U* = Unprotected, *P* = Protected to 520ºC at 90 minutes of fire exposure).

5 RESIDUAL STRUCTURAL TESTS

After fire testing, columns were allowed to cool, transported to the structural testing laboratories at the University of Edinburgh, UK, and stored in the structures laboratory (at about 20ºC and 50% relative humidity) for more than three months prior to structural testing.

Selected results of the residual structural tests are given in Table 2, including: the observed peak load (N_{test}); the axial deflection at peak load (δ_{axial}); the mid-span lateral deflection at peak load ($\delta_{lateral}$); and average axial strain at mid-height at peak load (ε_{ave}). The observed failure modes and the pre-peak axial rigidities of the columns are also given – approximated by a linear best fit of the load versus average axial strain at mid-height curve between the applied loads of 200 and 400 kN. Table 2 also shows the *residual strength index* (RSI) for each column tested after heating. The RSI is defined as the ratio of the tested strength (N_{test}) to the strength of an identical unheated column ($N_{ambient}$); i.e. RSI = $N_{test}/N_{ambient}$.

5.1 Overall structural response

The data in Table 2 show that, as expected, the severity of exposure to elevated temperatures significantly affected the observed axial failure load (N_{test}), the axial stiffness (k_{cfs}), as well as both axial (δ_{axial}) and lateral ($\delta_{lateral}$) deflections. The measured axial failure loads for unheated (sections x-x-x-N-N), fire-exposed but protected (sections x-x-x-(I/S)-C), and fire-exposed and unprotected (sections x-x-x-(I/S)-N) columns decreased in order with exposure to increasingly severe peak temperatures; these are presented in Table 1 and Figure 5. This is clearly evident in Figure 6, which gives total applied load versus axial and lateral deformations of circular (Figure 6a) and square (Figure 6b) CFS columns with FIB infill in unheated, unprotected, and protected cases that are otherwise identical, and shows the reduction in axial load capacity. The effect of increasingly severe peak temperature similarly reduces the axial stiffness, as shown in Figure 6 where reductions in the slope of the load deflections curves are evident as the peak temperature increases. Similarly, a clear reduction of k_{cfs} and axial deflections at peak load is evident as peak temperatures increase. Table 2 and Figure 6 clearly show that the fire protected CFS sections were able to retain between 60% and 90% of their ambient load capacity; an improvement of more than 30% as compared to unprotected sections which retained between 40% and 60% of their ambient load capacity.

The specific impacts of the varied parameters are discussed sequentially in the following sections.

Table 2: Recorded loads, deflections and strains at peak, failure modes, and pre-peak axial stiffness measured during post-fire residual structural tests.

Column	Test data[a]						RSI[b]	
	N_{test}[1]	δ_{axial}[2]	$\delta_{lateral}$[3]	ε_{ave}[4]	Failure mode[5]	k_{cfs} *(kN/mm)*[6]	$N_{ambient}$[7]	N_{test} /$N_{ambient}$
S-10-F-N-N	1949	15.7	-8.2	-2394	GB	127	1949	--
S-5-F-N-N	1467	14.4	-4.7	-2688	LBt	104	1467	--
S-10-F-I-N	1082	10.3	-3.7	-625[c]	GB	114	1949	0.56
S-5-F-I-N	617	8.0	-3.7	-4344	GB	90	1467	0.42
S-5-F-S-N	576	7.7	-3.8	-1960	GB	85	1467	0.39
S-5-F-I-C	1243	12.9	-4.2	-1514	LBt	108	1467	0.85
S-5-F-S-C	1215	13.3	-4.9	-1587	LBt	97	1467	0.83
C-10-F-N-N	1772	15.7	-10.0	-2700	GB	137	1772	--
C-8-F-N-N	1664	14.8	-10.0	-2870	GB	112	1664	--
C-5-F-N-N	1372	13.4	-8.3	-1761	GB/LBm	122	1372	--
C-5-H-N-N	1346	14.6	-10.2	-3051	GB	91	1346	--
C-10-F-I-N	1061	9.7	-3.7	-992	GB	121	1772	0.60
C-8-F-I-N	813	8.6	-3.4	-1012	GB	108	1664	0.49
C-5-H-I-N	583	10.3	-4.2	-3988	GB	66	1372	0.42
C-5-F-I-N	591	7.4	-4.0	-1116	GB	91	1346	0.44
C-5-F-S-N	601	7.6	-5.2	-1566	GB	96	1346	0.45
C-10-F-I-C	1241	11.0	-4.8	-1214	GB	123	1772	0.70
C-8-F-I-C	1285	12.8	-5.8	-2106	GB/LBm	114	1664	0.77
C-5-H-I-C	1192	13.4	-12.5	-3379	GB/LBm	109	1346	0.89
C-5-F-I-C	714	9.6	-5.8	-1537	LBq/GB	94	1372	0.52
C-5-F-S-C	795	9.6	-3.9	-2081	LBq/GB	100	1372	0.58
C-5-F-I-C(14d)	764	8.9	-5.3	-1360	LBq/GB	104	1346	0.57
C-5-F-I-C(28d)	741	9.2	-4.3	-1631	LBm/GB	92	1346	0.55
C-5-F-I-C(75)	833	12.5	-13.9	-3121	GB	97	1346	0.62
C-5-F-I-C(120)	835	11.2	-8.9	-2499	GB	95	1346	0.62

[a] Results at peak load for [1] load, [2] axial deflection, [3] mid-height lateral deflection, [4] average strain, and [5] failure mode (GB = global buckling, LB = local buckling of the steel tube), and [6] pre-failure axial stiffness; [b] RSI = residual strength index, with [7] $N_{ambient} = N_{test}$; [c] strain gauge failure.

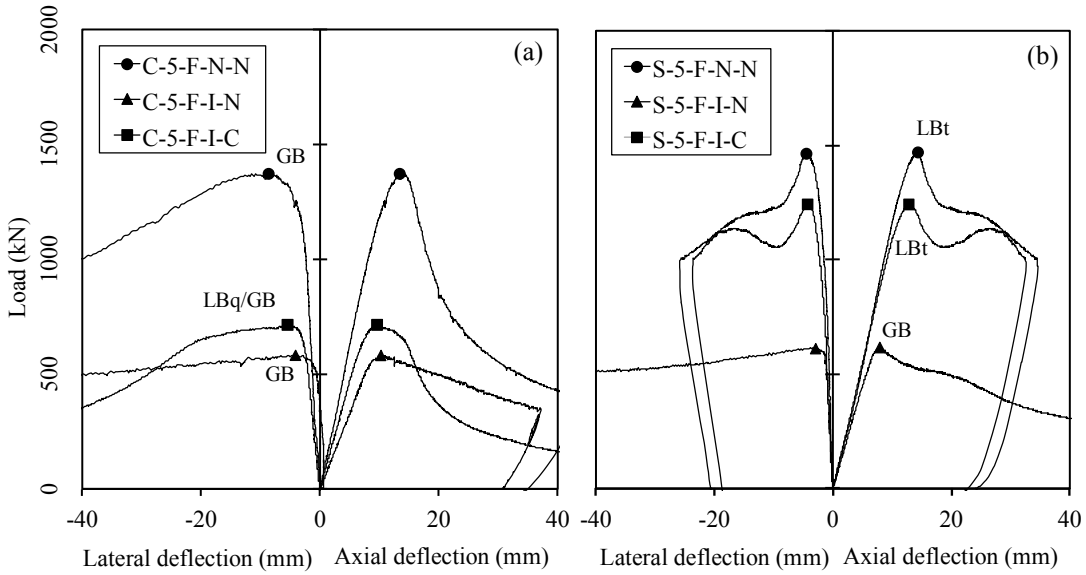

Figure 6 - Total applied load versus axial and lateral deflections for (a) C-5-F-x-x and (b) S-5-F-x-x columns tested either without fire exposure, unprotected and fire-exposed, and protected and fire-exposed (GB = global buckling, LBq = local buckling at quarter height, LBt = local buckling at the top).

5.2 Failure modes

Failure of the columns was due to 'buckling' in all cases, however initiation of failure was either through global buckling, leading to the formation of a local buckle near the columns' mid-height, or through local buckling away from the mid-height, leading to localised failure and preventing global buckling. In most cases a global buckling deformation mode occurred first, and resulted in the formation of a local buckle close to column mid height. In some cases the local buckle formed away from the column mid height (typically near the top of the column). Comparatively lower failure loads were observed for columns that failed due to local buckling away from mid-height, as compared with those that initially displayed a global buckling deformation state.

A representative selection of failure modes and post failure deformed shapes observed during testing is given in Figure 7. Circular CFS sections failed either by: (1) global buckling as in Figure 7(a); (2) local buckling as in Figure 7(c); or (3) global buckling leading to local buckling of the steel tube as in Figure 7(b). Global buckling failure modes (1) and (3) were observed in all tests of circular sections

apart from C-5-F-I-C, C-5-F-S-C, C-5-F-I-C(14d), and C-5-F-I-C(28d), all of which were protected, 5 mm wall thickness columns that failed by local buckling at approximately their quarter-heights, as shown in Figure 7(e). Local buckling failures occurred at these locations due to the thermocouple fixing method employed in these tests (refer to Figure 3). The fixings inhibited the consolidation of the concrete below the quarter height in these four columns, creating small air voids within the concrete core, as well as locally reducing the steel area due to four small (2mm diameter) holes that were drilled through the steel tubes at these locations to attach the thermocouple frames. The voids created by poor consolidation reduced the effective load bearing cross-section of the CFS columns, increasing the stresses in the reduced areas of both steel and concrete, and are very likely to have initiated these local buckling failures. If no concrete was present, for instance, at the quarter height cross-section, then the plastic capacity of the cross-section at that height is solely dependent on the steel. In the case of the C-5-F-x-C sections, for example, this would result in plastic axial capacities of approximately 680 kN.

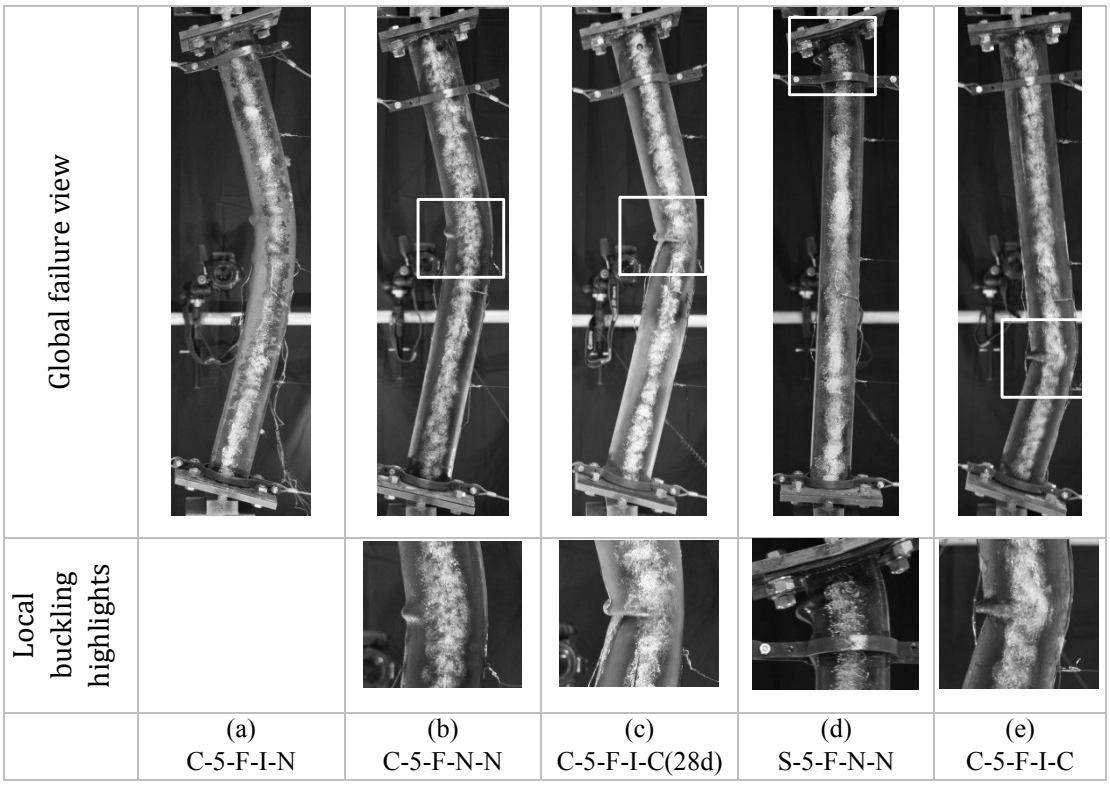

Figure 7. Typical deflected shapes and observed failure modes: (a) global buckling (GB); (b) global buckling followed by local buckling (GB/LB); (c) mid-height local buckling (LBm); (d) local buckling at top (LBt); and (e) local buckling (LBq) at quarter height.

Local buckling was observed in square section tests S-5-F-I-C, S-5-F-S-C, and S-5-F-N-N, all with 5 mm wall thickness, in the region of required moisture venting holes near the tops of the steel tubes (refer to Figure 1), as shown in Figure 7(d). This may be due to the reduced cross-sectional area of steel at this location, leading to stress concentrations and initiating failure. The local buckling failure load-deflection profiles can be seen in Figure 6(b) for the S-5-F-I-C and S-5-F-N-N columns, and shows that after the initial local buckling failure of the column, a secondary peak in axial capacity is observed due to the complex failure modes observed near the top of the columns. Unprotected fire-exposed columns S-5-F-I-N, S-5-F-S-N and S-10-F-I-N failed in global buckling, since the highly thermally damaged concrete core in these columns had a much lower residual strength. Thus, the residual axial/flexural stiffness of these columns was insufficient to prevent global buckling before the steel yielded around the venting holes. Specimen S-10-F-N-N had a capacity greater than 2000 kN, which exceeded the capacity

of the testing frame; however, a global buckling failure mode was observed to be initiating at the maximum load when the test was halted.

Few obvious trends were otherwise apparent in the failure modes in terms of correlating them to the different test parameters varied in the study, other than the fact that the sections with smaller steel wall thickness appeared to be more prone to local buckling, as should be expected. As discussed below the different failure modes played an important role in both the ultimate load capacity of the respective CFS columns, and their observed load versus deflection responses.

6 EXPERIMENTAL PARAMETRIC STUDY

6.1 Cross-section shape

Figure 8 (along with Figure 6) attempts to isolate the influence of cross-sectional shape (circular or square) on the overall response and RSI of CFS columns with 5 mm wall thickness and FIB infill. Figure 8 clearly shows a higher peak load capacity for protected square sections as compared to protected circular sections, suggesting that the protection was more effective for the square columns. This would result in lower peak temperatures within these cross-sections. However this is not corroborated by the peak temperature data given in Table 1 and Figure 5, and the difference in peak load capacity for the protected sections is instead a result of the observed failure mode; protected Column C-5-F-I-C failed by local buckling at quarter height (due to poor consolidation), compared to failure by local buckling at the top of S-5-F-I-C (due to reduced steel cross-sections around vent holes). This prevents direct comparisons for the protected sections. However, based on a comparison between the unexposed and unprotected columns in Figure 8, it would appear that square CFS sections may more sensitive to elevated temperature exposure from a residual capacity perspective, when they fail by global buckling; Column S-5-F-N-N failed by local buckling at its top, whereas S-5-F-I-N failed by global buckling. This is likely because square columns experience comparatively less confinement than circular ones (refer to Figure 1), and are

therefore less able to rely on the core concrete for residual strength contributions. Additional testing would be needed to confirm this hypothesis.

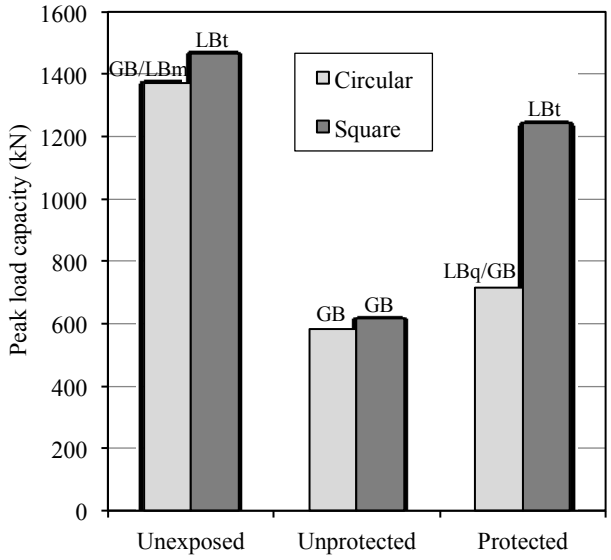

Figure 8 - Effect of cross sectional shape on capacity of CFS sections with 5 mm wall thickness and FIB infill subjected to the ISO 834 [11] **standard fire (failure modes noted).**

6.2 Steel tube thickness

Figure 9 shows observed load versus axial and load versus lateral deflection responses for C-x-F-I-N and C-x-F-I-C sections. Figure 10 provides a comparison of RSI values for both unprotected and protected sections with varying wall thickness, with FIB infill and exposed to the ISO 834 standard fire [11]. For both circular and square unprotected sections in Figure 10, all of which failed by global buckling, there is clear trend of decreased RSI with decreased steel tube thickness. This is likely due to the fact that columns with larger wall thickness are more dependent on the mechanical properties of the steel than the core concrete, and that steel is proportionally much less sensitive to elevated temperature exposure in terms of its ability to retain its mechanical properties on cooling. Furthermore, as shown in Figure 5, the wall thickness has no obvious effect on the temperatures experienced in the cross sections, thus columns with proportionally more steel cross sectional area (i.e. larger wall thickness) can be expected to have superior RSIs. This trend is less clear for the protected columns; however in this case the difference in

failure mode make the comparisons more difficult. It should be expected that a similar trend would be observed as for the unprotected sections, however less pronounced due to the milder peak temperatures experienced in these sections.

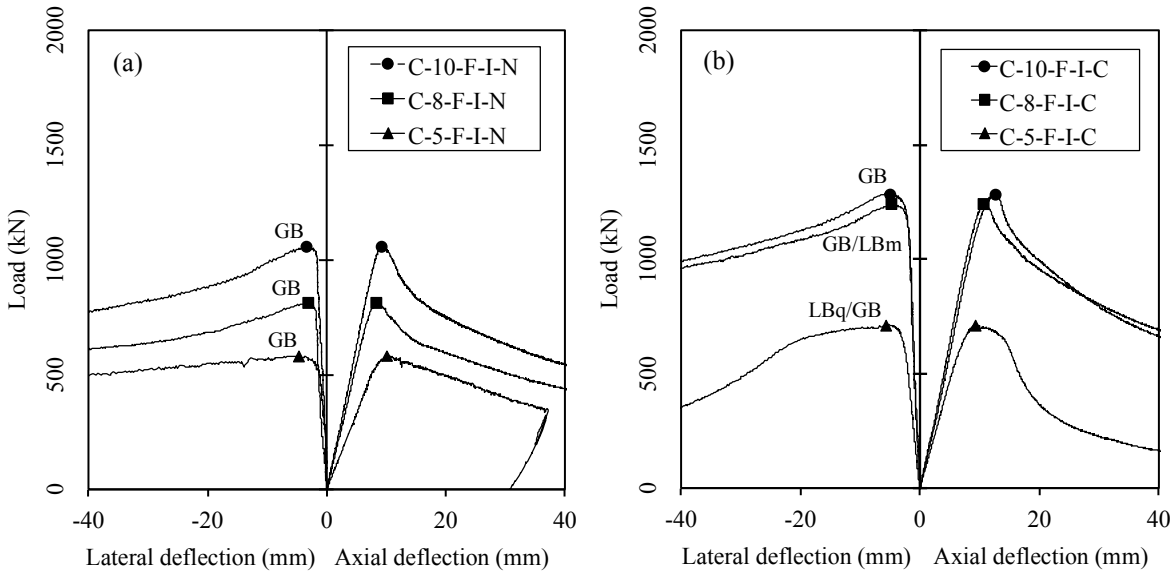

Figure 9 - Effect of steel tube wall thickness on residual load versus axial/lateral deformation response of (a) unprotected and (b) protected circular cross-section CFS columns.

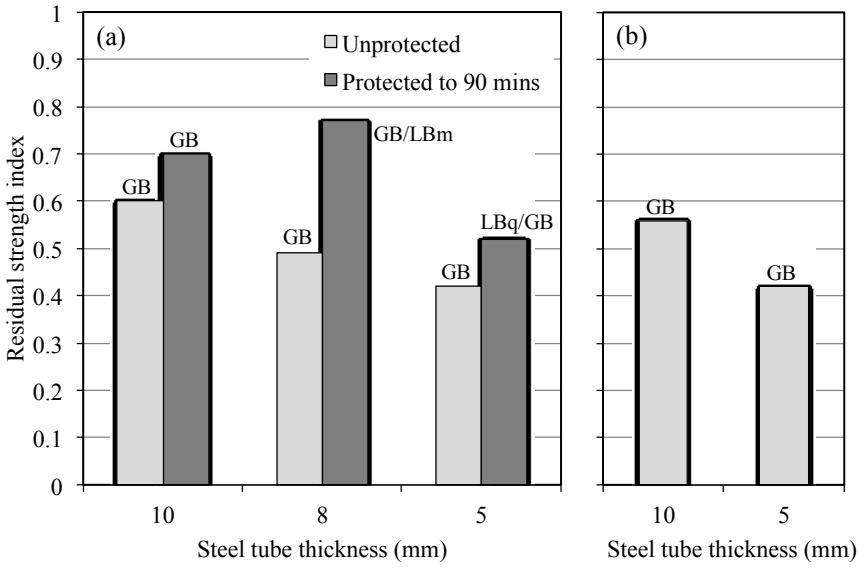

Figure 10 - Effect of steel tube wall thickness on RSI for (a) circular columns and (b) square columns, with FIB infill subjected to the ISO 834 [11] **standard fire (failure modes noted, see Table 2).**

6.3 Concrete infill type

Figures 11a and 11b show load-deflection relationships for C-5-F-x-x and C-5-H-x-x columns, filled with either FIB or HSC infill, respectively. Figure 12 isolates the effect of concrete infill type on peak axial load capacity for unheated, unprotected, and protected circular columns with 5 mm steel wall thickness. Interestingly, the concrete infill type had no obvious effect on the load deflection relationships for CFS columns, particularly given the complicating influences of variable failure modes in some cases. The only obvious change in response is seen by comparing C-5-F-I-C and C-5-H-I-C, where load versus deflection responses are markedly different; this is clearly due to the different failure modes experienced – these being premature local buckling failure and global buckling failure, respectively. The reasons for the local buckling failures at quarter height are due to a combination of poor consolidation of the infill concrete and the presence of small holes in the steel tube required to position thermocouples for measuring concrete core temperatures during the furnace tests, as previously described. In any case, the effect of infill concrete type (FIB or HSC) appears to be minimal or non-existent based on the data collected.

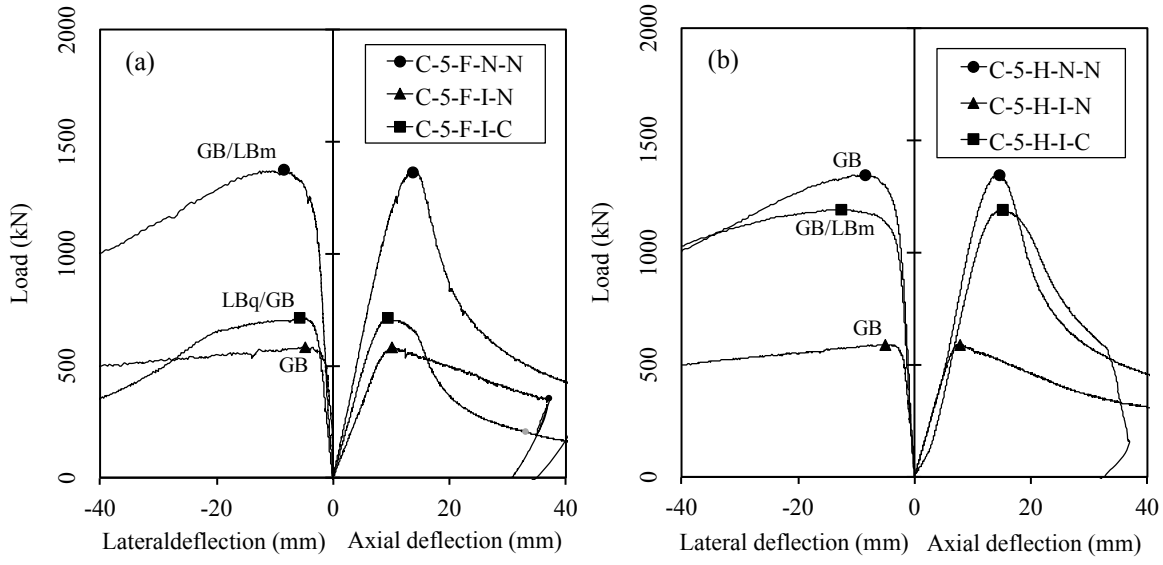

Figure 11 - Comparison of residual load versus axial/lateral deformation response of (a) fiber reinforced concrete infilled and (b) high strength concrete infilled 5 mm wall thickness circular cross-section columns.

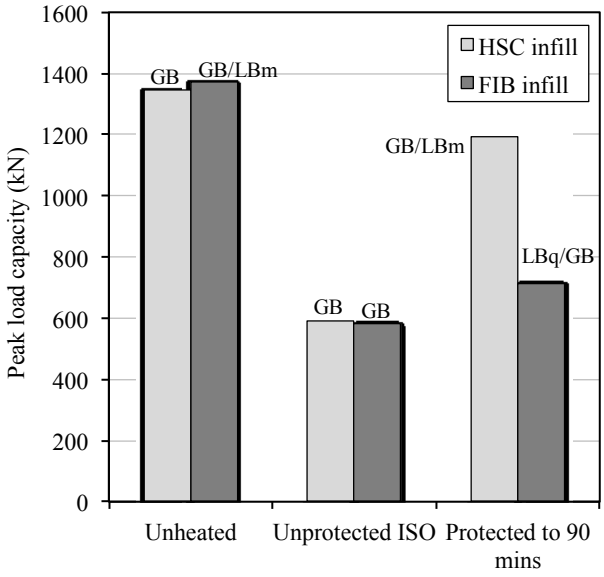

Figure 12 - Effect of concrete infill type on axial load capacity (unheated, unprotected, and protected circular columns with 5 mm steel wall thickness).

6.4 Type of Fire Exposure

Figure 13 isolates the effect of the type of fire exposure (ISO 834 or smouldering) on RSIs for circular and square, unprotected and protected, FIB-filled 5 mm wall thickness columns. For both unprotected and protected circular CFS sections, a mild trend of increasing RSI for columns subjected to the (slightly less severe) smouldering curve. This mild trend is reversed for the square sections; however, in both cases this may be coincidental given that the temperatures shown in Table 1 suggest no obvious differences in the peak temperature experienced by identical columns under these two different fire exposures, regardless of the section shape.

It is noteworthy that while Figure 13 appears to suggest that the RSIs of the protected square sections were vastly superior to those of the circular sections; this is an artifact of the fact that both of these sections failed by local buckling at the top, as did Column S-5-F-N-N. Such comparisons are therefore effectively meaningless from a post-fire residual capacity perspective.

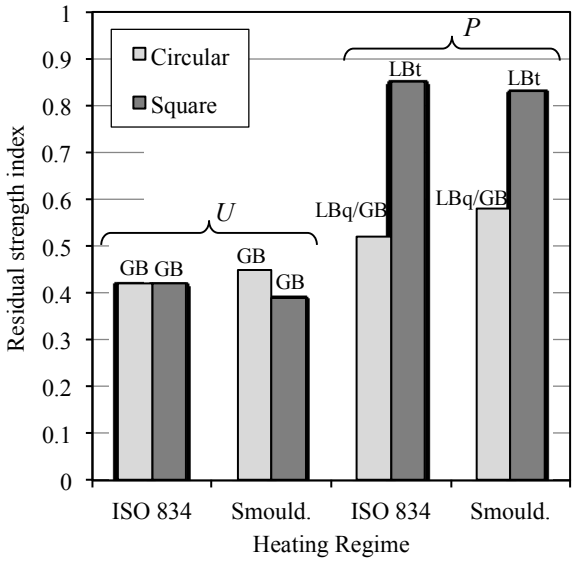

Figure 13 – Effect of type of fire exposure on RSI for circular and square, unprotected and protected, FIB-filled, 5 mm wall thickness CFS columns (*U* = Unprotected, *P* = Protected to 520°C at 90 minutes of fire exposure).

6.5 Concrete age and protection thickness

Columns C-5-F-I-C(14d) and C-5-F-I-C(28d) were exposed to an ISO-834 heating scenario 14 and 28 days after casting the concrete to evaluate the impact of the age of the infill concrete on; a) their response to heating; b) the effectiveness of the intumescent fire protection during furnace testing; and c) to some extent their RSI. The maximum temperatures observed at various depths (Table 1) and the performance of the intumescent coating showed very similar results for the young age concrete compared to specimens with concrete aged for 6 months, i.e. C-5-F-I-C. The RSIs for these three sections are shown in Figure 14a. Due to the occurrence of local buckling failure modes for these columns, generalizations are difficult to make, although no obvious trends were apparent, either in terms of their thermal or structural responses.

Figure 14b shows the RSI values for the two specimens that had intumescent fire protection dry film thicknesses (DFTs) designed and applied on the basis of required fire resistance times of 75 minutes C-5-F-I-C(75) and 120 minutes C-5-F-I-C(120), respectively. Both of these columns failed in global buckling and achieved similar maximum temperatures throughout their cross-sections. Thus, similar

capacities, and load-deflection and load-strain relationships were observed. A similar response was seen for C-5-F-I-C, which had a DFT designed for 90 minutes fire resistance however failed by local buckling at its quarter height, likely causing a slightly lower RSI evident in Figure 14b. In general, neither the concrete age at the time of testing nor the design fire resistance of the fire protection system obviously influenced the RSIs observed.

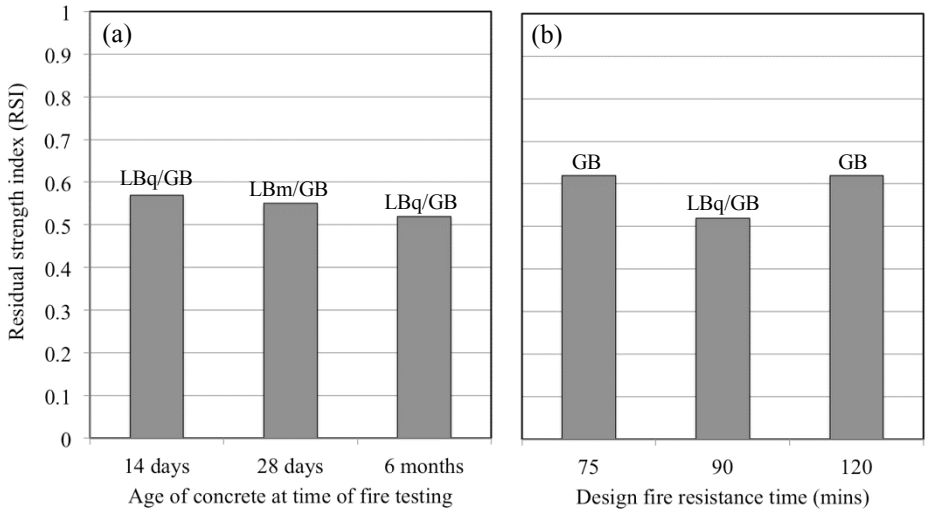

Figure 14 - Effect of (a) concrete infill age at the time of testing and (b) design fire resistance time on RSI for protected circular CFS columns with 5mm steel wall thickness.

7 PREDICTING POST-FIRE RESIDUAL CAPACITY

Residual strength predictions are presented in this section to assess whether common structural analysis methods for CFS columns can, with knowledge of the distribution of maximum exposure temperatures over a cross section, accurately predict their post-fire residual load capacity. Three different analysis methods are compared herein, along with Han et al.'s [5, 6] predictive model (Figure 2).

In all methods assessed the columns' cross-sections were discretised into a single steel layer and six concrete layers, and each layer was prescribed a uniform peak exposure temperature by parabolic interpolation of temperatures measured during the fire tests (and given in Table 1). Interpolated temperatures at the midpoint of each layer were assumed to apply over the entire layer. The steel tube

temperature was assumed to be uniform throughout the tube. Once the peak temperature for each layer was approximated, Han et al.'s [5, 6] temperature dependent stress-strain relationships for concrete and steel presented in Figure 1, which are the only constitutive models currently available in the literature for the post-heating residual response of confined concrete in compression, were applied for the steel tube and each concentric concrete layer, before analysis by each of the three methods described below is performed.

Several methods can be used to calculate the residual strength of a CFS column. In the current study three common, simplified methods are considered. The advantage of these methods over those previously suggested by Han and Huo [5] is that they can be applied to CFS columns of theoretically any size, and that they can be used to predict the post-fire capacity of CFS columns exposed to any fire (i.e. non-standard fire) and with any form of applied fire insulation (provided that the peak temperatures over the cross-section can be determined).

7.1 Method 1: Eurocode 4 Annex H approach (N_{pred1})

Method 1 represents the approach suggested by Annex H of Eurocode 4 [1] for fire resistance predictions of CFS columns at high temperature; however using 'residual' constitutive properties (Figure 1) for the constituent materials rather than 'hot' properties. This is an incremental axial strain approach that considers failure by both cross-sectional crushing and global buckling. The strain is assumed to be uniform over the cross-section (i.e. no bending and minimal load eccentricity). The axial strain is then increased incrementally to find the failure load, N_{pred1}. This is assumed to be reached when the total axial load over the cross-section, determined as the summation of the areas of each annular element multiplied by the current stress in that layer at the current axial strain and accounting for the post-fire reductions in mechanical properties (shown in Figure 1), reaches a maximum or equals the buckling resistance of the column, again at the current axial strain level and based on a summation of the post-fire residual flexural

rigidities of each of the annular elements. Details of the calculations are avoided here but are provided by Rush [21] and in Eurocode 4 [1].

7.2 Method 2: Eurocode 4 plastic capacity of cross-section (N_{pred2})

Method 2 essentially follows the recommended procedures for ambient temperature structural analysis and design of CFS columns from Eurocode 4 [17]; however using residual constitutive properties (Figure 1). Eurocode 4 [17] provides a simplified approach that can be used to determine CFS column capacity for ambient temperature design, and this can be modified for post-fire residual analysis. In this method, the plastic resistance of the section, N_{pred2}, is calculated by summing the maximum possible resistance of each layers (i.e. material peak strength after exposure to high temperature times cross-sectional area for each annular element).

7.3 Method 3: Eurocode 4 buckling resistance of cross-section (N_{pred3})

Method 2 above (N_{pred2}) is only applicable to short columns, so for the post-fire capacity of a potentially slender CFS section (as in the current study) the values of N_{pred2} are reduced to account for buckling. This is achieved by initially calculating the elastic critical buckling load, and, along with the maximum plastic resistance, the column's relative slenderness. The relative slenderness is used with buckling curves given in Eurocode 4 [17] to calculate the CFS column's buckling reduction factor, and thus its capacity, N_{pred3}, according Eurocode 4.

7.4 Prediction results

Table 3 and Figure 15 compare the performance of the three above approaches at predicting the post-fire residual capacity of the columns tested in the current study, with the solid diagonal line representing a perfect prediction. In Table 3, negative % errors are under-predictions (i.e. conservative) and positive % errors over-predictions (i.e. unconservative). In Figure 15, points lying above the solid line represent

over-predictions whereas points lying below the line represent under-predictions. Also included in Table 3 and Figure 15 are the mean predictive abilities of the respective approaches (represented by diagonal lines in Figure 15). The failure loads predicted using method 1, N_{pred1}, were on average over-predicted by 2% whilst the methods 2 and 3 on average over-predicted by 24% and under-predicted by 19%, respectively, when considering all specimens. When only global failure modes are considered (i.e. no local buckling at either the top or at quarter height) the mean predictive abilities of methods 1 and 3 under-predicted by 3% and 23% respectively, whilst method 2 over-predicted by 14%. The variance of the errors for each of the methods reduced when local buckling was not considered, from 17%, 28%, and 17%, to 11%, 17%, 10%, for methods 1, 2, and 3, respectively.

Table 3: Comparison of recorded and predicted failure loads

Column	Test data[a]			Predicted failure loads			% error		
	N_{test}[1]	Failure mode[5]	*RSI*	N_{pred1}	N_{pred2}	N_{pred3}	N_{pred1}	N_{pred2}	N_{pred3}
S-10-F-N-N	1949	GB	--	1913	2235	1217	-2%	15%	-38%
S-5-F-N-N	1467	LBt	--	1267	1607	834	-14%	9%	-43%
S-10-F-I-N	1082	GB	0.56	1055	1092	745	-3%	1%	-31%
S-5-F-I-N	617	GB	0.42	566	623	424	-8%	1%	-31%
S-5-F-S-N	576	GB	0.39	560	621	424	-3%	8%	-26%
S-5-F-I-C	1243	LBt	0.85	1144	1553	803	-8%	25%	-35%
S-5-F-S-C	1215	LBt	0.83	1111	1535	794	-9%	26%	-35%
C-10-F-N-N	1772	GB	--	1893	2204	1434	7%	24%	-19%
C-8-F-N-N	1664	GB	--	1647	1955	1256	-1%	18%	-25%
C-5-F-N-N	1372	GB/LBm	--	1245	1535	950	-9%	12%	-31%
C-5-H-N-N	1346	GB	--	1245	1535	950	-8%	14%	-29%
C-10-F-I-N	1061	GB	0.60	958	990	778	-10%	-7%	-27%
C-8-F-I-N	813	GB	0.49	793	825	649	-2%	1%	-20%
C-5-H-I-N	583	GB	0.42	510	562	441	-12%	-3%	-24%
C-5-F-I-N	591	GB	0.44	511	563	441	-14%	-5%	-25%
C-5-F-S-N	601	GB	0.45	526	592	459	-12%	-1%	-24%
C-10-F-I-C	1241	GB	0.70	1664	1962	1311	34%	58%	6%
C-8-F-I-C	1285	GB/LBm	0.77	1403	1716	1133	9%	33%	-12%
C-5-H-I-C	1192	GB/LBm	0.89	1039	1364	862	-13%	14%	-28%
C-5-F-I-C	714	LBq/GB	0.52	1007	1340	850	41%	88%	19%
C-5-F-S-C	795	LBq/GB	0.58	1014	1347	853	28%	69%	7%
C-5-F-I-C(14d)	764	LBq/GB	0.57	1017	1349	854	33%	76%	12%
C-5-F-I-C(28d)	741	LBm/GB	0.55	957	1287	825	29%	74%	11%
C-5-F-I-C(75)	833	GB	0.62	827	1090	729	-1%	31%	-12%
C-5-F-I-C(120)	835	GB	0.62	819	1080	725	-2%	29%	-13%
						Average % error	2%	24%	-19%
						Standard deviation of % errors	17%	28%	17%
						Average % error exclude. LBq and LBt	-3%	14%	-23%
						Standard deviation of % errors exclude. LBq and LBt	11%	17%	10%

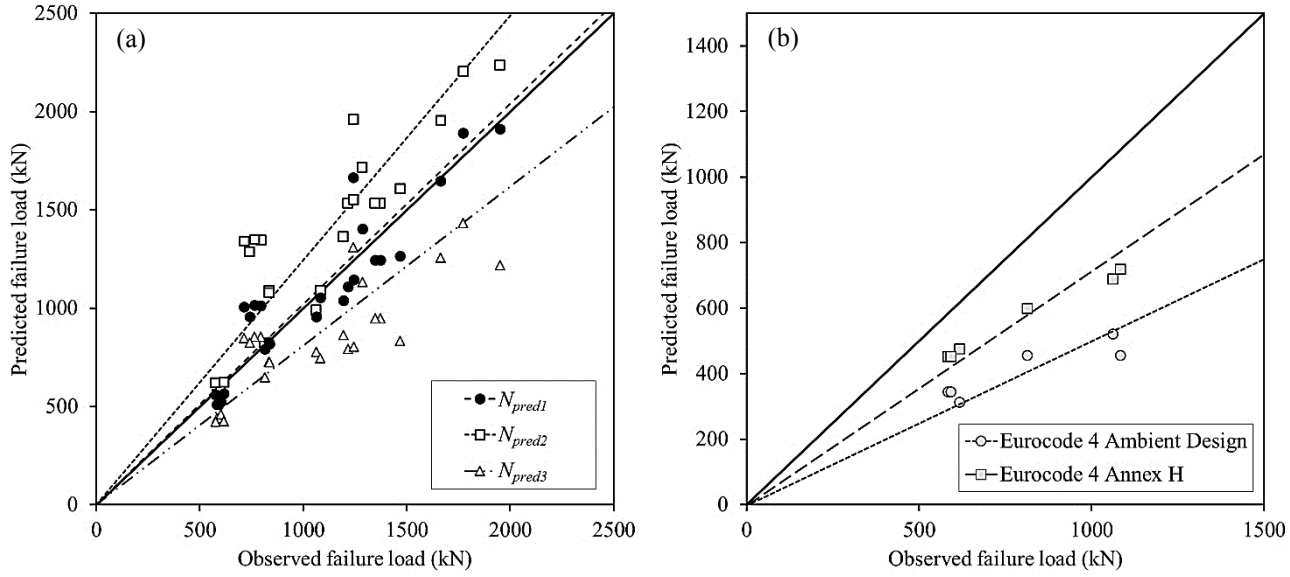

Figure 15 – Predicted versus observed post-fire residual axial load bearing capacity for all columns tested in the current study, for (a) the three predictive methods discussed in this section and (b) the RSI equations proposed by Han and Huo [5]

7.5 Han and Huo [5] residual strength index predictions

As previously discussed, Han and Huo [5] also provide a method for determining the post-fire residual capacity of unprotected CFS columns exposed to standard fires. In their approach the residual strength is determined by multiplying the ambient strength of the column by the RSI; the variation in RSI with time of fire exposure is shown in Figure 2 for the unprotected columns tested in the current study. This leads to post-fire residual strengths of 0.364 and 0.376 of the columns' ambient capacity, for the circular and square columns, respectively. Figure 15b shows that this yields highly conservative residual capacity predictions, assuming that the ambient temperature capacity can be approximated using the Eurocode 4 procedures for ambient temperature design [17] (i.e. N_{pred3} for the x-x-x-N-N columns). If the Eurocode 4 Annex H approach [1] is used to predict the ambient temperature capacity (i.e. N_{pred1} for the x-x-x-N-N columns), then the Han and Huo predictions are, on average, only slightly conservative. This may support a change to the Annex H approach even for the case of ambient temperature design of CFS

columns; however this would necessitate additional analysis on the part of designers as compared with the existing Eurocode 4 ambient temperature design method.

8 CONCLUSIONS

This paper has presented results and analysis of 25 post-fire residual axial compressive tests on fire-exposed CFS columns that had been exposed to different severities of heating in furnace tests; this was accomplished either by application of fire protection in the form of intumescent paint, or by using a smouldering fire curve rather than the ISO 834 [11] standard fire. Based on the residual test data and analysis presented herein, the following conclusions can be drawn:

- As expected, as the maximum temperatures experienced within the CFS sections increases, the residual axial failure load and axial stiffness of the CFS columns decreases.
- Supplemental fire protection can help CFS sections to retain their capacity and rigidity after fire. Protected columns, in which much lower maximum temperatures were experienced, retained up to 30% more of their ambient structural capacity compared with the unprotected columns; in these cases the residual strength of the column was as low as 40% of the ambient capacity after 120 minutes of ISO 834 fire exposure.
- The columns failed either by global or local buckling. For the circular sections local buckling was only observed in the sections with 5 mm wall thicknesses and where the severity of the temperatures experienced in the cross-section were reduced by the presence of intumescent coatings. For the square sections local buckling was observed even when the section had not been exposed to fire. The various failure modes observed make some test parameter comparisons difficult or impossible, and it is noteworthy that the 'premature' local buckling failure modes that were observed in the tests presented herein are not routinely considered by structural engineers during design.

- The load-deflection and load-strain relationships (not presented in detail) of different CFS columns were found to be similar, of course depending on the specific failure mode experienced.
- Square CFS sections maybe more sensitive to elevated temperature exposure from a residual capacity perspective, when they fail in a global buckling mode.
- There is a reasonably clear trend of decreased RSI with decreased steel tube thickness, for columns that are otherwise identical.
- The effect of infill concrete type (FIB or HSC) appears to be minimal or non-existent based on the data collected.
- There are no obvious differences in the peak temperature experienced by identical columns, either protected or unprotected, under either ISO 834 or smouldering fire exposures, regardless of the section shape.
- Neither the concrete age at the time of testing nor the design fire resistance of the fire protection system obviously influenced the RSIs obtained.
- In terms of predicting the RSI for fire-exposed CFS columns, a method (Method 1 herein) based on the Eurocode 4 Annex H approach [1] was found to be the best predictor on average over-predicting by 2%. An alternative method (Method 2) based on the maximum theoretical plastic compressive sectional resistance, was unconservative by 24%, whereas a third method (Method 3) based on a modification of the Eurocode 4 [17] ambient temperature design procedure for CFS columns was conservative by 19%.
- Han and Huo's [5] method for determining the residual strength of unprotected CFS columns exposed to standard fires was found to be highly conservative when the ambient temperature capacity of the CFS column was approximated using the Eurocode 4 procedures for ambient temperature design [17]. If the Eurocode 4 Annex H approach [1] is used to predict the ambient capacity, then the Han and Huo residual strength predictions are only slightly conservative on average.

9 ACKNOWLEDGEMENTS

The authors would like to acknowledge the generous support of Ove Arup and Partners, The Ove Arup Foundation, The Royal Academy of Engineering, the Engineering and Physical Sciences Research Council, and the School of Engineering at the University of Edinburgh, part of the Edinburgh Research Partnership in Engineering (ERPE).

10 REFERENCES

[1] CEN, "BS EN 1994-1-2:2005: Eurocode 4 — Design of composite steel and concrete structures — Part 1-2: Genreal rules - Structural fire design," Brussels, Belgium, 2008.

[2] V. Kodur, "Guidelines for fire resistant design of concrete filled steel HSS columns: State-of-the-art and research needs," *Int. J. Steel Struct.*, vol. 7, no. 3, pp. 173–182, 2007.

[3] L. H. Han, J. S. Huo, and Y. C. Wang, "Compressive and flexural behaviour of concrete filled steel tubes after exposure to standard fire," *J. Constr. Steel Res.*, vol. 61, no. 7, pp. 882–901, Jul. 2005.

[4] L. H. Han, Y. F. Yang, H. Yang, and J. S. Huo, "Residual strength of concrete-filled RHS columns after exposure to the ISO-834 standard fire," *Thin-walled Struct.*, vol. 40, no. 12, pp. 991–1012, 2002.

[5] L. H. Han and J. S. Huo, "Concrete filled hollow structural steel columns after exposure to ISO-834 standard fire," *J. Struct. Eng.*, vol. 129, no. 1, p. 68, 2003.

[6] H. Yang, L. H. Han, and Y. C. Wang, "Effects of heating and loading histories on post-fire cooling behaviour of concrete-filled steel tubular columns," *J. Constr. Steel Res.*, vol. 64, no. 5, pp. 556–570, May 2008.

[7] J. S. Huo, G. Huang, and Y. Xiao, "Effects of sustained axial load and cooling phase on post-fire behaviour of concrete-filled steel tubular stub columns," *J. Constr. Steel Res.*, vol. 65, no. 8–9, pp. 1664–1676, Aug. 2009.

[8] V. K. R. Kodur, N. K. Raut, X. Y. Mao, and W. Khaliq, "Simplified approach for evaluating residual strength of fire-exposed reinforced concrete columns," *Mater. Struct.*, vol. 46, no. 12, pp. 2059–2075, 2013.

[9] J. Barrington, D. Dickson, L. Bisby, and T. Stratford, "Strain Development and Hoop Strain Efficiency in FRP Confined Square Columns Jason," *10th Int. Symp. Fiber Reinf. Polym. Reinf. Reinf. Concr. Struct.*, pp. 9.1–9.20, 2011.

[10] T. T. Lie and B. Celikkol, "Method to calculate the fire resistance of reinforced concrete columns with rectangular cross section," *ACI Struct. J.*, vol. 90, no. 1, 1991.

[11] ISO, “ISO 834: Fire resistance tests-elements of building construction,” Geneva, Switzerland, 1999.

[12] D. Rush, “Fire performance of unprotected and protected concrete filled structural hollow sections,” University of Edinburgh, 2013.

[13] CEN, “BS EN 13381-8:2010: Test method for determining the contribution to the structural fire resistance of structural members; Part 8: Applied reactive protection to steel memebrs,” Brussels, Belgium, 2010.

[14] S. J. Hicks, G. M. Newman, M. Edwards, and A. Orton, “Design guide for concrete filled columns,” Corus Tubes, Corby, Northants, 2002.

[15] CEN, “BS EN 1991-1-2:2002 Eurocode 1- Actions on structures; Part 1-2: General Actions - Actions on structures exposed to fire,” Brussels, Belgium, 2009.

[16] CEN, “BS EN 13381-6:2012 - Test methods for determining the contribution to the fire resistance of structural members: Part 6: Applied protection to concrete filled hollow steel columns,” Brussels, Belgium, 2012.

[17] CEN, “BS EN 1994-1-1:2004; Eurocode 4 : Design of composite steel and concrete structures — Part 1-1: General rules and rules for buildings,” Brussels, Belgium, 2009.

[18] Y.-H. Li and J.-M. Franssen, “Test results and model for the residual compressive strenght of concrete after a fire,” *Journal of Structural Fire Engineering*, vol. 2, no. 1. pp. 29–44, 2011.

[19] CEN, “BS EN 1992-1-2:2004 - Eurocode 2 : Design of concrete structures — Structural fire design,” Brussels, Belgium, 2010.

[20] BSI British Standards, “BS EN 1993-1-2:2005; Eurocode 3 : Design of steel structures — Part 1-2: General rules — Structural fire design,” 2010.

[21] D. Rush, L. Bisby, A. Jowsey, A. Melandinos, and B. Lane, “Structural performance of unprotected concrete-filled steel hollow sections in fire: A review and meta-analysis of available test data,” *Steel Compos. Struct.*, vol. 12, no. 4, pp. 325–350, Apr. 2012.